

# 3D Bioprinting for Cancer Modeling and Personalized Medicine

Subjects: Cell & Tissue Engineering

Contributor: Nicolas Germain, Melanie Dhayer, Philippe Marchetti

Tumor cells evolve in a complex and heterogeneous environment composed of different cell types and an extracellular matrix. Current 2D culture methods are very limited in their ability to mimic the cancer cell environment. Various 3D models of cancer cells have been developed, notably in the form of spheroids/organoids, using scaffold or cancer-on-chip devices. However, these models have the disadvantage of not being able to precisely control the organization of multiple cell types in complex architecture and are sometimes not very reproducible in their production, and this is especially true for spheroids. Three-dimensional bioprinting can produce complex, multi-cellular, and reproducible constructs in which the matrix composition and rigidity can be adapted locally or globally to the tumor model studied. For these reasons, 3D bioprinting seems to be the technique of choice to mimic the tumor microenvironment *in vivo* as closely as possible.

Keywords: 3D bioprinting ; 3D printing ; bioink ; cancer ; cell biology

---

## 1. 3D Bioprinting at a Glance

### 1.1. Introduction

Additive manufacturing has been a major breakthrough in construction technologies and has been considered “the third industrial revolution” [1]. Additive manufacturing, commonly known as 3D printing, allows for building parts one layer at a time from a 3D computer model, allowing for rapid design optimization and customization. Because of these interesting properties, medical applications have been quickly developed: 3D-printed prostheses, implants, anatomical models, etc. [2][3]. The ease of use and speed of prototyping has even allowed for quick responses to medical needs during the COVID-19 pandemic [4][5][6].

The rapid development of this technology has required the development of new materials capable of being printed, in particular plastics, but also metals, ceramics, and elastomers. Traditionally, the materials used for 3D printing in medicine are made of inert and acellular materials, such as plastics [7]. Among those materials, some are bio-compatible and can thus be used for implantation [8]; other materials are degradable and are used as guides for soft tissue reconstruction, e.g., breast reconstruction after cancer surgery [9]. Recently, a new field of research in 3D printing has emerged: 3D bioprinting. Three-dimensional bioprinting uses 3D-printing technology to print cells and a supportive matrix (called bioink) altogether, ultimately printing a living tissue [10]. Bioinks have been defined by Groll et al. as “a formulation of cells suitable for processing by an automated biofabrication technology that may also contain biologically active components and biomaterials” that could be resumed as cell-containing materials [11]. Three-dimensional bioprinting, while promising, raises a large number of concerns and challenges, in particular the development of biocompatible bioinks and their integration into the human body; however, it seems to be a proper tool for complex tissue *in vitro* modeling [12].

### 1.2. Bioprinting Technologies

The first bioprinting technique was described in 2003 by Boland et al., who used an inkjet-based technique to print 2D tissue constructs [13]. Since this first experiment, numerous bioprinting technologies have been created and can be classified into three main categories depending on the type of cell deposition: drop-based (e.g., inkjet or laser bioprinting), filament-based (e.g., extrusion bioprinting), and plane-based (e.g., digital light processing (DLP)/stereolithography (SLA) bioprinting) (Table 1).

**Table 1.** Most commonly used bioprinting technologies.

Type of Technology	Example of Printing Method	Advantages	Disadvantages	Cell Density	Average Cell Viability	Crosslinking	References
Droplet-based	Laser	Very high accuracy and resolution Low shear stress Very expensive	Only low-viscosity bioinks Only 2D patterns (limited high)	Low (less than 10 million per mL)	High	Depends on biomaterial used	[14][15]
	Inkjet	High accuracy Low shear stress					[16][17]
Filament-based	Worm drive Pneumatic Syringe/piston	Large panel of bioinks available Low cost Highly tunable	Higher shear stress and lower cell viability than other bioprinting technologies	High (more than 10 million per mL)	Medium/high depending on nozzle and pressure	Depends on biomaterial used	[13][18][19][20]
Plane-based/Volumetric	DLP/SLA	Fast for large and complex 3D models Very high accuracy	Few bioinks available Waste of bioink due to its conception	High (more than 10 million per mL)	High	Photocurable by DLP/SLA technology	[21][22][23][24][25]

Nowadays, the most-used technology is the filament-based one, with different extrusion mechanisms: pneumatic, piston, and screw-driving (**Figure 1**). Extrusion-based techniques resulting in filament deposition are nowadays the most used as they can quickly produce scaffolds of a resolution down to 100  $\mu\text{m}$  in an affordable and relatively simple way [18].

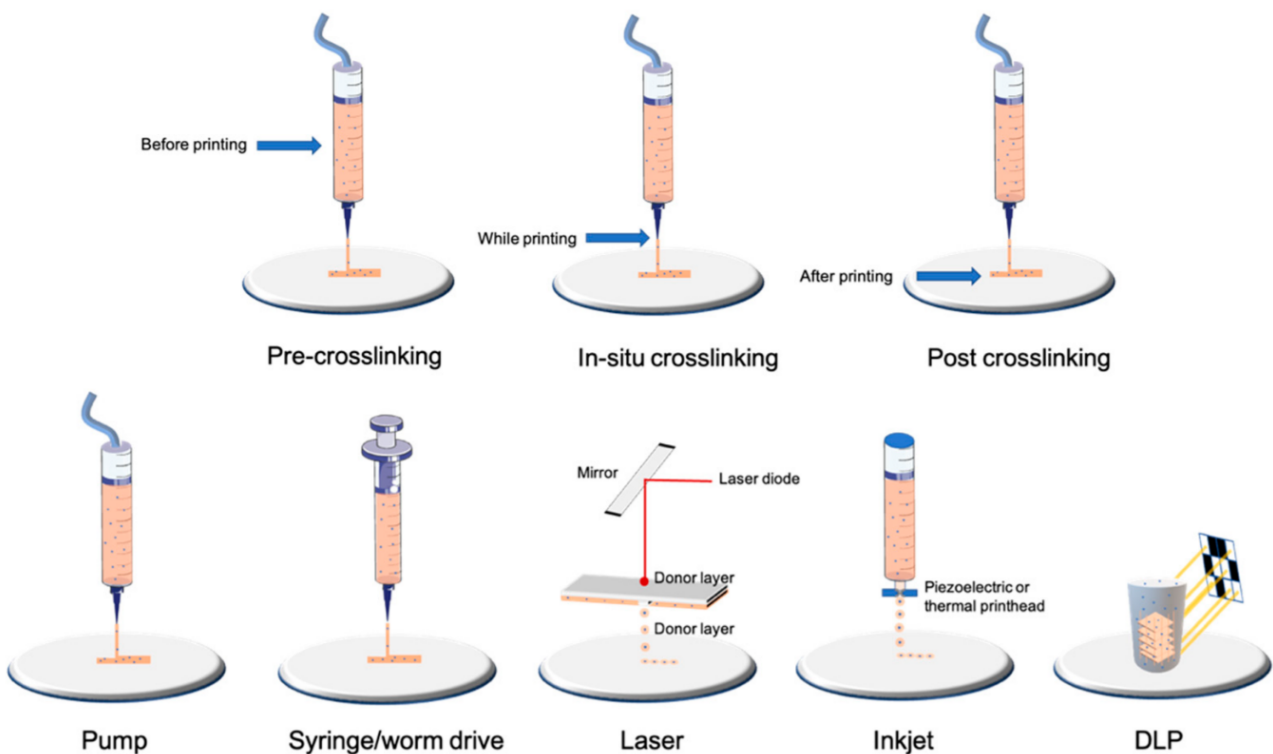


**Figure 1.** Examples of bioprinting and crosslinking technologies.

In researchers' opinion, nowadays, this technology is the easiest to implement; many manufacturers offer machines with multiple extrusion printheads (some printheads may even use inkjet-based printing techniques (see below for details)) all in a tabletop format and with a user-friendly interface at reasonable prices. This technology is also compatible with almost all bioink formulations [19].

Droplet-based techniques are consistent with the discontinuous printing of microdroplets and thus a high resolution (for review, see [26]). Inkjet printing is the most common technology used for droplet generation and consists of a piezoelectric

or thermal actuator that allows the precise deposition of the droplets down to 50  $\mu\text{m}$  [16][17]. Laser-based droplet deposition allows single-cell deposition and, as a non-contact method, is responsible for low shear stress and thus excellent viability; the drawback is the expensive price of this type of 3D printer [14][15]. There are also other less-used approaches, such as acoustic- or valve-based droplet bioprinting technologies [27][28]. Even if the droplet generation (surface tension) and breaking combined with the force with which it will be projected onto the printing plate can reduce cell viability, drop-based approaches allow higher cell viability than filament-based ones (>85%).

This technology, although it brings a precision that extrusion-based ones cannot have, only allows the printing of 2D patterns. This can be useful to precisely include cells in a pre-existing 3D matrix but not for large-scale constructions.

Plane-based 3D printing is mainly consistent in DLP and SLA technology (for review, see [21][22]). In SLA technology, photopolymerization is achieved through a laser beam scanning the surface of a liquid bioink, whereas in the DLP technique, polymerization is achieved by a digital micromirror device (DMD) or by a liquid crystal display (LCD) [23]. Volumetric bioprinting is a technique derived from those light-based techniques and can enable the creation of entire objects at once, which allows free-form architecture bioprinting that cannot be achieved with other technologies [24].

Those techniques have a high resolution down to 25  $\mu\text{m}$  and speed in producing large and complex volumes; however, this technique requires a large volume of bioink, a significant part of which will not be polymerized [25].

Despite these interesting characteristics, particularly the speed of printing large volumes and the precision, it is not the easiest to implement this technology, particularly because of the lack of compatible bioinks and its running cost. It is, however, interesting for printing complex microfluidic structures.

## 2. Characterization of Cells after Bioprinting

To evaluate the success of a bioprinting model, one of the most important parameters to assess is the viability and metabolic activity of the cells. Indeed, it is necessary to find the adequate printing parameters that allow for obtaining the structural integrity of the hydrogel so that it is reproducible and especially viable. These parameters must be determined for each type of bioink and even for each concentration. Printing parameters, such as the bed or cartridge temperature, pressure, and printing speed, will modify the viscosity of the gel, which will affect the shear stress exerted on the cells and, therefore, their viability. This is also impacted by the way the hydrogels are crosslinked.

A plethora of techniques is available to characterize cells after bioprinting to determine the size and organization of the constructs, cell viability, and metabolism and the level of gene and protein expression [29][30] (Table 3, Figure 2). The size and shape of the constructs must be adapted to the technique used. For example, microscopic analysis does not require many cells, in contrast to cytometry, molecular biology technics, or spectrometric analysis. After adaptation, the usual techniques used in conventional 2D culture can be applied.

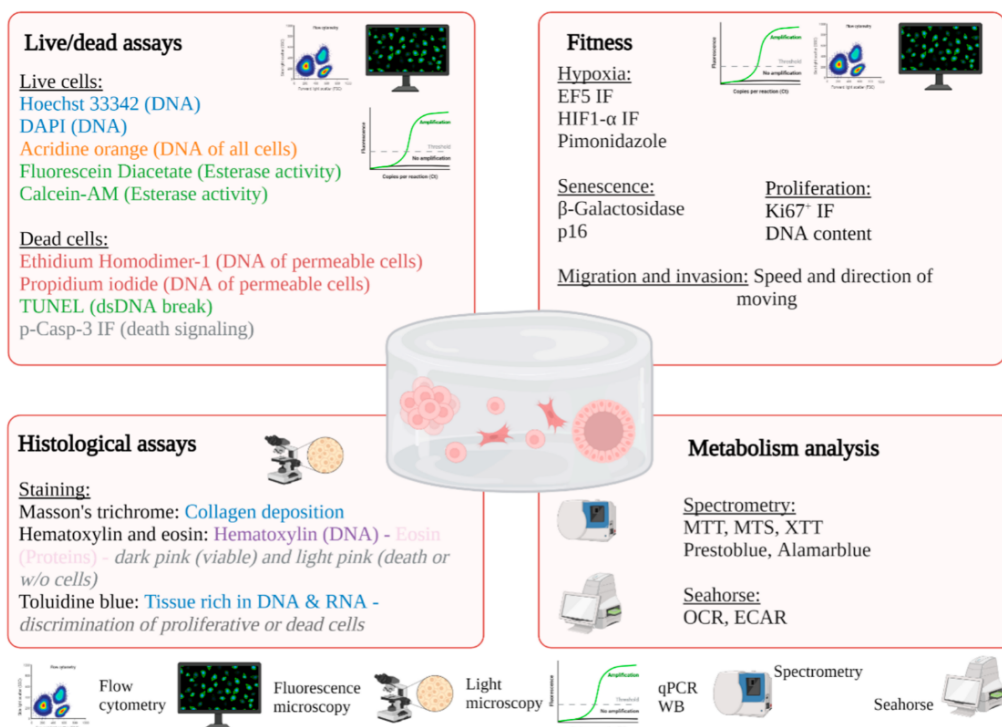


**Figure 2.** Examples of possible analysis of 3D bioprinted constructs.

## 2.1. In Situ Characterization of Cells

The advantage of using techniques where the cells are embedded in the hydrogel allows for avoiding artifacts related to the dissociation of the hydrogel.

### 2.1.1. Light Microscopy

Microscopy is particularly interesting in the characterization of hydrogels because it allows the structure of the construct to be preserved, as well as the cell–cell interactions. It allows access to the size and morphology of cells that could assemble into spheroids or in a native tissue organization. Phase-contrast microscopy allows for monitoring cell proliferation and growth over time without inducing toxicity [31][32][33]. However, because the cells are alive, the acquisition time should not be too long to avoid inducing cell death. This technique is only possible for optically transparent hydrogels. For example, the cell-ink bioink composed of alginate and cellulose nanofibril is opaque and does not track cells without prior fluorescent labeling or end-point histological analysis.

Histological analysis requires sample preparation, including fixing, cutting, and staining [32][33][34]. The preparation steps for sectioning are very important. Dehydration for paraffin embedding tends to shrink the size of the sample and is therefore not recommended for structural or organizational measurements [35]. In addition, if the hydrogel pores are not completely filled with paraffin, this will promote folding during sectioning and detachment of the sample from the section. However, the advantage of this technique is the possibility of having thin sections (up to 5  $\mu\text{m}$  thick). In contrast, cryosection preserves the hydrogel structure, particularly with polyvinyl alcohol (PVA) and optimum cutting temperature (OCT) preparation. However, the sections are thicker, and more aspecific markings can be observed with a protein-based cryoprotectant solution [36]. Using resins favors the preservation of structures but makes it more difficult to perform histological stains [37]. Finally, it is possible to proceed directly to histological staining without cutting to visualize the cells on the surface of the hydrogel. Depending on the structures of interest, different stainings are available: Masson's trichrome (TM) stains collagenous structures in blue (fibrosis, for example); hematoxylin (DNA) and eosin (proteins) illuminate viable zones in dark pink and dead zones in clear pink; and, finally, toluidine blue highlights the zones rich in RNA and DNA. Trypan blue is used to stain dead cells [38]. Quantification of chromatic staining can be difficult on thick samples, so the use of fluorescence microscopy is a good alternative.

### 2.1.2. Fluorescence Microscopy

Fluorescence microscopy is used to label subcellular structures, such as the cytoskeleton (F-actin), mitochondria (MitoTracker), nuclei (Hoechst), or other types of organelles or proteins [39][40][41][42]. Standard immunofluorescence or biomarker labeling protocols can be applied to the hydrogel, although the times of the different labeling steps should be increased or even improved using mechanical agitation or a vacuum. Observation of the organization and viability of cells as a function of the position or shape of the hydrogel is only possible under microscopy. Using markers or antibodies coupled to fluorescent probes, it is possible to determine whether cells are dying (p-casp3), proliferating (KI67<sup>+</sup> or DNA), entering in senescence (p16 or  $\beta$ -galactosidase), or in a hypoxic environment (HIF1- $\alpha$ , EF5, pimonidazole). Numerous fluorescence assays for dead/live cells are described in **Table 2**; however, the most commonly used combination of fluorochromes is calcein AM stain for esterase activity (live cells) and propidium iodide for permeable and therefore dead cells. It is possible to combine one of these two markers with Hoechst3342 or DAPI; however, this is not possible in all types of hydrogels, such as alginate, which shows strong auto-fluorescence from the UV channel. An easy-to-use marker for studying cell morphology is phalloidin labeling of F-actin, which is particularly interesting in models for studying mechanotransduction as a function of support stiffness, for example [38][43][44][45].

**Table 2.** Examples of bioinks and their applications in cancer research.

Material	Type of Bioink	Bioprinting Technology	Tissue Engineering Model	Cancer Models	Advantages	Drawbacks	Type of Crosslinking	References	
Bioink derived from natural biomaterials	Alginate-based	Natural polysaccharide (brown algae)	Drop-based Filament-based	Vascular, cartilage, bone, neural tissue, fibroblast, and many more	Drug delivery Cancer stem cell research Breast cancer, melanoma, and many more cancers Tumor spheroids	Low cost Good printability Excellent biocompatibility	Poor cell adhesion Fast degradation	Ionic	<a href="#">[46][47][48][49]</a> <a href="#">[50][51][52]</a>
	Gelatin-based	Natural protein (bovine skin and tendon)	Drop-based Filament-based Plane-based	Vascular, cartilage, bone, muscle, fibroblast, and many more	Cholangiocarcinoma, bladder cancer, and many more cancers Tumor spheroids	Excellent biocompatibility Low-cost High cellular adhesion	Low viscosity at room or higher temperatures Need a temperature-controlled (cooled printhead) and a cooled printbed Low mechanical strength (higher if blended with methacrylate)	Chemical Thermal UV Covalent Enzymatic	<a href="#">[53][54][55]</a> <a href="#">[56][57][58]</a>
	Cellulose and nanocellulose-based	Natural polysaccharide obtained from the biosynthesis of plants or bacteria	Filament-based	Cartilage and bone	Drug delivery Gastric, cervical, pancreatic, and many more cancers	Great similarity with ECM Excellent biocompatibility	Low viscosity for cellulose nanocrystals Mainly used mixed with other natural biomaterials	Enzymatic UV	<a href="#">[59][60][61][62]</a> <a href="#">[63]</a>
	Matrigel	Solubilized basement membrane matrix secreted by Engelbreth-Holm-Swarm (EHS) mouse sarcoma cells	Filament-based Drop-based	Vascular, liver, bone, lung, and many more	Tumor spheroids Many types of cancer	Most used material in cancer research Excellent biocompatibility Very well characterized for organoid/spheroid formation	Cannot be used alone due to its complex rheological behavior and low mechanical properties Limited use in vivo due to its mouse tumor origin Expensive High batch variability	Thermal	<a href="#">[64][65][66][67]</a> <a href="#">[68]</a>
	Collagen-I-based	Natural protein (rat tail or bovine skin and tendon)	Drop-based Filament-based	Hard tissues (bone, osteochondral, cartilage) Skin, cardiovascular, and liver tissues; nervous system; and cornea	Tumor spheroids Neuroblastoma, breast cancer	Excellent biocompatibility High cellular adhesion Minimal immunogenicity Excellent printability Enzymatically degradable Mechanical and structural properties close to native tissue	Low shape fidelity	pH Thermal	<a href="#">[69][70][71][72]</a>
	Hyaluronic-acid-based	Natural polysaccharide (bacterial fermentation or animal products)	Filament-based	Hard tissues (bone, osteochondral, cartilage)	Tumor spheroids Melanoma, breast cancer	Excellent biocompatibility Highly tunable (wide variety and high degree of potential chemical modifications) Interact with cell receptors	Poor mechanical strength Mainly used mixed with other natural biomaterials	Depends on the other biomaterial/chemical modifications Physical or covalent	<a href="#">[73][74][75][76]</a>

Material	Type of Bioink	Bioprinting Technology	Tissue Engineering Model	Cancer Models	Advantages	Drawbacks	Type of Crosslinking	References
Agarose-based	Natural polysaccharide derived from red seaweed	Filament-based	Bone, vascular, neural, and adipose tissue	Leukemia	Good biocompatibility Great similarity with ECM Thermo-reversible gelling	Poor cell survival if not blended with another biomaterial Poor printability (needs high temperature for dispensing (70 °C) and gels at low temperatures)	Thermal Ionic	[65][77][78]
Fibrin-based	Natural protein (human plasma)	Filament-based Drop-based	Muscular, neural, skin, and adipose tissue, wound healing model	Drug release Glioblastoma	High shape fidelity (depending on fibrinogen-thrombin concentration) Excellent biocompatibility Enzymatically degradable	Medium cell adhesion Low mechanical properties	Enzymatic (fibrinogen-thrombin)	[79][80][81]
Silk-derived	Natural protein (bombyx mory)	Filament-based	Hard tissues (bone, osteochondral, cartilage), vascular tissue	Drug delivery	High shape fidelity Low Cost Good biocompatibility	Lacks cell-binding domains Medium cell viability Needs other supportive material for cell proliferation (alginate, gelatin, etc.) Poor printability performance	Enzymatic Physical	[82][83][84][85]
Gellan gum	Natural polysaccharide	Filament-based	Hard tissues (bone, osteochondral, cartilage), brain-like structures	Drug delivery	Excellent biocompatibility Low cost Rapid gelation	Poor printability performance	Thermal	[86][87][88]

For high-resolution microscopy, confocal imaging is the reference method for studying cells embedded in the hydrogel. The disadvantage is the necessity to print thin film constructs on suitable substrates. Indeed, without a cleaning technique, only 100 µm-thick constructs can be imaged. Furthermore, these hydrogels should preferably be printed on glass coverslips to favor high-resolution imaging. The risk is that the hydrogel may become detached; to mitigate this, the silanization of the coverslips allows the covalent bonding of the gel with its support. To limit the constraints of confocal imaging, other microscopy techniques have been developed, such as light sheet imaging, thus possible to image large objects without a physical section with limited phototoxicity [39][40][41][42].

### 2.1.3. Electronic Microscopy

Electron microscopy provides nanoscale imaging, either scanning for the sample's surface or transmission for the internal structures [90][91]. These techniques allow the study of cell-cell or cell-ECM interactions but also cell death. However, the sample preparation steps can change the structure of the sample.

## 2.2. Characterization of Cells after Isolation or Lysis

### 2.2.1. Molecular Biology

For many applications in tissue engineering, it is necessary to be able to extract DNA, mRNA, or protein in order to monitor different cellular parameters such as differentiation or certain functions. It is also possible to determine proliferation and viability via the measurement of DNA concentration. This technique is interesting since it allows for knowing the number of cells per gel but also for normalizing the data obtained to the number of cells. However, it is critical to find the right technique to lyse the cells to recover the full amount of DNA. For example, for alginate gels, it is possible to use a commercial solution, the purelink genomic DNA mini kit [111]. For GelMA or agarose, the use of EDTA associated with proteases allows the recovery of cells from the gel in order to assay the DNA [44][45][112][113][114][115].

Conventional methods for 2D cell culture rely on two methods: either via the use of phenol/chloroform or with commercial kits using silica membranes in spin columns [116]. However, the inclusion of cells in hydrogels makes this step more difficult, and it presents more challenges that are technical. Indeed, the classical RNA extractions often do not allow for obtaining RNAs in sufficient quantity and/or quality for the subsequent performance of RTqPCR. Köster's team conducted a study to investigate homogenization methods and RNA extraction techniques based on the most commonly used hydrogels (alginate, gelatin, and agarose) on hMSC cells [117]. For this purpose, four homogenization techniques are deployed. Regardless of the type of hydrogel, homogenization techniques using liquid nitrogen or a rotor stator should be excluded, as the yield of RNA is very low. In contrast, the amount of RNA is much higher for techniques using the micro-homogenizer or enzymatic/chemical digestion. The technique of frozen liquid nitrogen crushed by an electric crusher seems to be relevant for GelMA-type homogenization [44][112]. For extraction, Köster's team shows that conventional commercial kits using silica membranes in spin columns do not provide a correct RNA yield for hMSC in alginate, gelatin, and agarose hydrogels [117]. However, other teams obtain satisfactory results with agarose-based or alginate hydrogels

[45][118]. Hot phenol (HP), TRIzol (TR), cetyltrimethylammonium bromide (CTAB), and LiCl (LC) techniques have a better RNA yield, but the LiCl technique gives poor PCR results (e.g., dominating additional band, PCR product with incorrect size or no PCR product). For the same reasons, the TRIzol technique is not adapted for 2D culture gels for Köster's team but it is for Cho's team. Cho's team's team of 3D hot phenol and CTAB seem to be the most suitable techniques; hot phenol gives the best RNA yield, and CTAB gives the best RNA quality (equivalent to 2D culture) and low endpoint Ct values ~20.

### 2.2.2. Flow Cytometry

It can also be interesting to sort cells to improve cell expansion or to analyze using flow cytometry as this allows many cells to be analyzed very quickly. For this purpose, enzymatic degradation is possible on matrices derived from natural products, such as collagenase for GelMA or collagen hydrogels, hyaluronidase for hyaluronic acid-based gels, or alginate lyase for alginate hydrogels. Some materials can also be degraded by physical techniques, such as photo-degradation [120]. This step is critical because a too-prolonged enzyme treatment can induce significant cell death or even alter the membrane receptors. The limitation of this technique also lies in the fact that hydrogels are required to recover the necessary number of cells after degradation [121]. The standard labeling protocols such as 2D culture can be used. Flow cytometry allows quantitative measurements of many parameters simultaneously, such as viability, proliferation, cell cycle, and uptake of anti-cancer agents. As for microscopy, live/dead tests based on calcein AM and ethidium are the most commonly used, with propidium iodide or BrdU for the cell cycle. It is also interesting to use this technique to identify subpopulations or maintenance of a phenotype, such as chronic lymphocytic leukemia cells on CD5<sup>+</sup>CD19<sup>+</sup>IgM<sup>+</sup> markers. The disadvantage of flow cytometry compared to microscopy is the loss of spatial information. To compensate for this, Beaumont's team developed a protocol based on the diffusion gradient of Hoechst 33342, which makes it possible to discriminate between internal and peripheral cells according to the intensity of Hoechst [122].

**Table 3.** Characterization technology of bioprinted constructs. Value of 3D bioprinting for cancer modelling. + for pros and - for cons.

Methods	Description	Pros and Cons	Markers	REF			
<b>Microscopy</b>							
Light	Phase contrast	Monitoring of proliferation and morphology of cells	+	• Nondestructive • No markers are added • Low cost • Easy with transparent gels (GelMA, matrigel) -:	• No possibility to identify subcellular structures • Difficult with opaque or non-transparent gels (e.g., alginate with nanocellulose)	Not suitable	[31] [32] [33]
	Bright field	The transmission of light is more or less attenuated depending on the density or marking of the sample	+	• Suitable for large samples -:	• Requires histological staining • Preparation of sample • Quantification of thick sample	Hematoxylin-eosin Masson's trichrome Trypan blue	[32] [33] [34]
Fluorescence	LSM Epifluorescence Confocal	The use of a fluorescent marker is necessary to highlight a subcellular structure; possibility of monitoring structures over time (if vital markers)	+	• Monitoring of many possible structures -:	• Requires cutting for oversized constructions for epi and confocal microscopy • Need to fix for certain markers • Important autofluorescence for chitosan or alginate/cellulose hydrogels in UV	Live/dead staining Or calcein AM/propidium iodide Or ethidium homodimer Active-caspase3/7 green Hoechst 33342 HIF1- $\alpha$ , Ki67	[39] [40] [41] [42] [123]

Methods	Description	Pros and Cons	Markers	REF
Electronic	Scanning	Surface is scanned with a beam of electrons, emitted signal provides images	Not suitable	[33]
	Transmission	The part of beam of electrons is transmitted into specimens allowed to obtain images	Not suitable	[33] [110]
Flow cytometry				
Flow cytometry	Analysis of physical parameters (size and granularity) for each cell but also the level of fluorescence	<ul style="list-style-type: none"> <li>+: • Quantitative analysis</li> <li>-: • Disaggregation can be a problem</li> <li>• Necessity to have a large cell number due to loss of cells during dissociation</li> </ul>	7-AAD CFSE	[33] [117]
Spectroscopy				
Spectrometry or fluorimetry	Production or utilization of a fluorescent or chromatic compound	<ul style="list-style-type: none"> <li>+: • Well-described for 2D culture and frequently used</li> <li>• Can be used for kinetic monitoring</li> <li>-: • Ensure that the efficiency is adapted for 3D</li> </ul>	ACP, LDH, prestoblue, alamar blue, DNA content	[43] [124] [125] [126]
Molecular biology				
RTqPCR Western blot	Quantification of gene expression at mRNA or protein level	<ul style="list-style-type: none"> <li>+: • Quantitative analysis</li> <li>• Easier by using the enzymatic method on natural inks (e.g., collagenase for GelMA or ColMA, hyaluronidase for hyaluronic acid)</li> <li>-: • Adaptation of the homogenization and extraction protocol to obtain an adequate quantity and quality of RNA/proteins for analyses</li> </ul>	Bax/Bcl2 HIF1- $\alpha$ , Ki67	[34] [110] [119]
Metabolism				
GC-MS (Gas chromatography-mass spectrometry)	Detection of molecules of interest according to their mass/charge ratio after ionization	<ul style="list-style-type: none"> <li>+: • Considerably less cellular material compared to NMR, high sensitivity,</li> <li>-: • Use of radioisotopes, complex sample preparation, high cost</li> </ul>	<sup>13</sup> C-Glucose	[127] [128]
NMR (nuclear magnetic resonance) spectroscopy	Determination of the composition of a sample by applying a magnetic field via the orientation of the nuclear spins of the atoms	<ul style="list-style-type: none"> <li>+: • High reproducibility, sample can be analyzed directly, low cost</li> <li>-: • Use of radioisotopes, low sensitivity</li> </ul>		[129] [130]
PET scan (positron emission tomography)	Injection of a radiographic tracer and monitoring by imaging to detect localization of [ <sup>18</sup> F]FDG	<ul style="list-style-type: none"> <li>+: • Classically used in medicine, monitoring over time</li> <li>-: • Low resolution (1.5 mm)</li> </ul>	[ <sup>18</sup> F]FDG	[125] [131]
Seahorse	Quantification of the oxygen consumption rate (OCR) and the extracellular acidification rate (ECAR)	<ul style="list-style-type: none"> <li>+: • High sensitivity (from 5000 cells, theoretically), possibility to test many conditions in parallel</li> <li>-: • Difficulties in normalizing results, limited number of injections, limited sample thickness</li> </ul>	Not suitable	[132] [133]

7-AAD: 7-ADDminoactinomycin; [<sup>18</sup>F]-FDG: 18F-2-Fluor-2-deoxy-D-glucose; ACP: acid phosphatase assay; CFSE: carboxyfluorescein succinimidyl ester; CTV: celltraceviolet; MTS: 3-(4,5-dimethylthiazol-2-yl)-5-(3-carboxymethoxyphenyl)-2-(4-sulfophenyl)-2H-tetrazolium; MTT: 3-(4,5-dimethylthiazol-2-yl)-2,5-diphenyltetrazolium

bromide; pNPP: p-nitrophenyl phosphate; PET: positron emission tomography; WST: water-soluble tetrazolium; XTT: 2,3-bis-(2-methoxy-4-nitro-5-sulphophenyl)-2H-tetrazolium-5-carboxanilide.

Actual models for cancer study range from in vitro traditional 2D cultures to in vivo models; most of the time, the complexity of the model goes hand in hand with the complexity of assaying the subsequent metabolism [134]. Three-dimensional bioprinting allows for adding high-complexity tissue modeling in a relatively user-friendly technology (Figure 3). Compared to the widely used organoid approach, 3D bioprinting allows, in an automated way, the creation of complex 3D structures with the precise and reproducible deposition of cells and matrices.

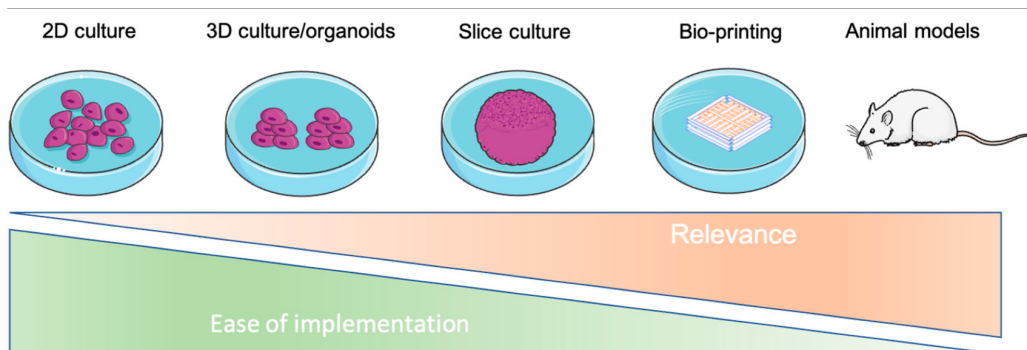


**Figure 3.** Relevance and ease of implementation of different research models.

Bioprinting is, therefore, an innovative approach to mimic the in vivo microenvironment of cancer cells as closely as possible (Figure 4). This has the advantage of producing more viable results that are closer to in vivo results, such as cell–cell or cell–ECM, or resistance to treatment as a function of the microenvironment. One could also imagine mimicking the tumor microenvironment for each patient (personalized medicine) or for a cohort (biobanks) to test their responses and resistance to the different therapeutic lines. New bioprinting methods have also made it possible to obtain a greater number of cancer stem cells, cells that are particularly difficult to maintain in vitro and incriminated in cancer relapse.

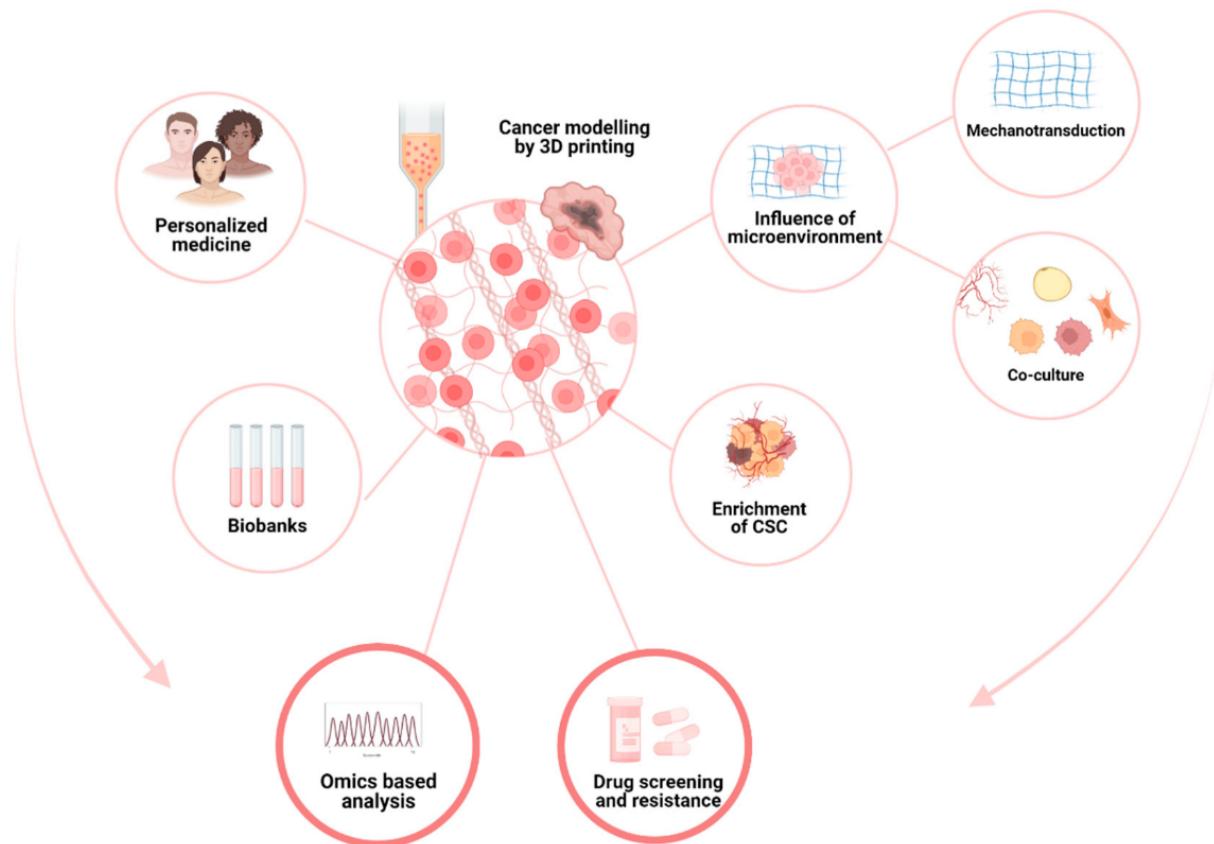


**Figure 4.** The value of bioprinting for oncology research.

## 2.3. Recapitulate Cancer’s Relation to the Microenvironment

### 2.3.1. Cells–ECM Interaction

For a long time, the study of cancers was solely based on the precise genetic, metabolic, and phenotypic analysis of single tumor cells, with tumor stroma being totally ignored [135]. Recently, there has been strong evidence of stroma–tumor

interactions related to tumor progression [136]. This cancer stroma is a complex framework of supportive tissue composed of the extracellular matrix (ECM), cells (such as fibroblasts and adipocytes), inflammatory and immune cells, and a specific vascularization. Thus, there are complex interactions between the stroma and the cancer cells: cancer cells can modify their stroma, and stroma can support tumor progression.

Adipocytes are a main component of the human body and are thus in the vicinity when tumorigenic events take place [137]. Complex crosstalk is then set up, in which phenotypical and functional modifications of both tumor cells and adipocytes occur. Adipocytes release fatty acids that can be oxidized in cancer cell mitochondria and thus provide energy through ATP in times of metabolic need [138]. In breast cancer, aberrant adipocytes called cancer-associated adipocytes (CAA) are known to promote the invasion and metastasis of breast cancer, in particular through the secretion of adipocytokines in the invasive front of the tumor [139]. Horder et al. bioprinted a breast cancer model with adipose-derived stromal cells (ADSC) [76]. ADSCs were differentiated into adipocytes within the hyaluronic acid gel and allowed the remodeling of the ECM with increased collagens I and IV and fibronectin expression, demonstrating the important interactions between cancer cells and adipose tissue.

Cancer-associated fibroblasts are another key component of the tumor microenvironment, notably through their capacity to remodel the extracellular matrix but also through direct cellular interactions via paracrine signals (exosomes, metabolites, and cytokines) with cancer and immune cells [140][141]. In a recent paper, Hanley et al. showed that CAF could be a potential target to overcome resistance to anti-PD1/PD-L1 and CTLA-4 immunotherapy [142]. Mondal et al. printed non-small cell lung cancer (NSCLC) patient-derived xenograft (PDX) cells and lung CAFs that allowed high viability and efficient crosstalk [143].

Spheroids have long been used to complexify tumor models, but despite their 3D structure, they are not sufficient to recapitulate the complexity of the microenvironment, notably due to the lack of multiple cell types and vascularization. Three-dimensional bioprinting allows for recapitulating the complexity of the tumor microenvironment, particularly through the precise deposition of several cell types, the ability to vary the type of matrix, and the ability to precisely set up vascularisation networks [144][145]. As reported by Samadian et al., ECM components and cells have a crucial role in the progression and spread of cancers, and 3D bioprinting allows for mimicking the tumor microenvironment at physical, cellular, and molecular levels [146]. The possibility of making sacrificial templates using sacrificial materials (e.g., pluronics F-127) allows the setting up of vessel-like structures that can be cellularized and perfused, improving nutrient availability [147]. Different strategies can be used for the printing of a vascular network that is recapitulated by Richards et al., but extrusion-based bioprinting is quite capable of printing complex networks (for review, see [148]).

### **2.3.2. Neoangiogenesis**

Angiogenesis is a normal mechanism by which new blood vessels can be generated. Angiogenesis is made up of different stages, including the degradation of the matrix via proteases and the migration and proliferation of endothelial cells to form new tubes that are anastomosed with pre-existing ones [149]. In a normal state, angiogenesis is mainly regulated by hypoxia, in particular through the hypoxia-inducible transcription factor (HIF) family [150]. To allow tumor growth, cancer cells will stimulate endothelial cells activity by releasing many soluble factors, such as EGF, FGF, and VEGF. Tumor-endothelial interactions are also essential in metastasis processes.

Three-dimensional bioprinting allows for studying the mechanisms at the origin of neoangiogenesis. As reported by Zervantonakis et al., 3D breast adenocarcinoma bioprinted models associated with microfluidics can recapitulate changes in the endothelial barrier caused by tumor–endothelial cells interactions and model the process of intravasation [151]. In a model of lung carcinoma, 3D bioprinting of a vascularized tissue allowed for exploring the molecular mechanisms of metastasis by using a gradient of angiogenic factors, such as EGF and VEGF, in printed programmable release capsules [152].

## **2.4. Mechanical Environment**

### **2.4.1. Mechanotransduction**

It has now been well-known for many years that cellular metabolism cannot be reduced to the functioning of an isolated cell. Cells grow and interact with their environment, notably via chemical and physical factors that can drive their fate. This mechanism of sensing, integrating, and responding to external signals is widespread in almost all living organisms. Chemical interactions mediated by soluble factors or cell–cell interactions have been extensively studied in the past; however, cell interactions with their environment and notably with the extracellular matrix (ECM) cannot be reduced to chemical stimuli. In recent years, physical cues have proved to be major regulators of the cell response to external stimuli, including the ability to sense external applied forces, rigidity, topography, and orientation [153][154][155]. The mechanism by

which these external physical stimuli are detected, transmitted to the cell, and converted into biochemical information is called mechanotransduction [156]. The detection of external stimuli, also called mechanosensing, depends on the nature of the signal and is particularly mediated through focal adhesion complexes (FAs) (composed of multiple mechanosensors, such as talin and vinculin), adherens junctions, and mechanically activated channels (e.g., Piezo) (for review, see [157]). The microenvironment can induce different physical and mechanical stresses on tumor cells. The cell can be subjected to three different types of mechanical stress: (i) tensile stress, related to the contraction of actomyosin during the stiffening of the ECM; (ii) compressive stress, due to the anarchic proliferation of cells in a confined space during tumor growth phases; and (iii) shear stress with blood and interstitial fluid pressure. Among the physical determinants of mechanotransduction, stiffness has proved to be a major regulator of cell metabolism. Stiffness is a term used to describe the force necessary to obtain the deformation of a structure [158]. In cell biology, the stiffness of a tissue is mainly derived from ECM composition and thus the proportion of its components that are mainly represented by fibrous-forming proteins, e.g., collagens, elastin, and fibronectin (for review, see [159]). Among them, hyaluronan acid and collagens are the main determinants of ECM stiffness. Information derived from ECM stiffness can then be converted by the cells and influence their fate, particularly through changes in their metabolism [160]. One remarkable feature of cancer cells is the capacity to change their metabolism to adapt to the harsh conditions of their specific tumor environment and adapt to the aberrant signaling induced by oncogenes or tumor suppressors [161]. Thus, there is a complex dialogue between the cancer cells and the tumor microenvironment as the cells can change their composition and stiffness, and in turn, the change in stiffness can lead to changes in cancer cell metabolism.

---

## References

1. Huang, S.H.; Liu, P.; Mokasdar, A.; Hou, L. Additive Manufacturing and Its Societal Impact: A Literature Review. *Int. J. Adv. Manuf. Technol.* 2013, 67, 1191–1203.
2. Ho, C.M.B.; Ng, S.H.; Yoon, Y.-J. A Review on 3D Printed Bioimplants. *Int. J. Precis. Eng. Man.* 2015, 16, 1035–1046.
3. Diment, L.E.; Thompson, M.S.; Bergmann, J.H.M. Clinical Efficacy and Effectiveness of 3D Printing: A Systematic Review. *BMJ Open* 2017, 7, e016891.
4. Belhouideg, S. Impact of 3D Printed Medical Equipment on the Management of the Covid19 Pandemic. *Int. J. Health Plan. Manag.* 2020, 35, 1014–1022.
5. Choong, Y.Y.C.; Tan, H.W.; Patel, D.C.; Choong, W.T.N.; Chen, C.-H.; Low, H.Y.; Tan, M.J.; Patel, C.D.; Chua, C.K. The Global Rise of 3D Printing during the COVID-19 Pandemic. *Nat. Rev. Mater.* 2020, 5, 637–639.
6. Tino, R.; Moore, R.; Antoline, S.; Ravi, P.; Wake, N.; Ionita, C.N.; Morris, J.M.; Decker, S.J.; Sheikh, A.; Rybicki, F.J.; et al. COVID-19 and the Role of 3D Printing in Medicine. *3D Print. Med.* 2020, 6, 11.
7. Yan, Q.; Dong, H.; Su, J.; Han, J.; Song, B.; Wei, Q.; Shi, Y. A Review of 3D Printing Technology for Medical Applications. *Engineering* 2018, 4, 729–742.
8. Nuseir, A.; Hatamleh, M.M.; Alnazzawi, A.; Al-Rabab'ah, M.; Kamel, B.; Jaradat, E. Direct 3D Printing of Flexible Nasal Prosthesis: Optimized Digital Workflow from Scan to Fit. *J. Prosthodont.* 2019, 28, 10–14.
9. Faglin, P.; Gradwohl, M.; Depoortere, C.; Germain, N.; Drucbert, A.-S.; Brun, S.; Nahon, C.; Dekiok, S.; Rech, A.; Azaroual, N.; et al. Rationale for the Design of 3D-Printable Bioresorbable Tissue-Engineering Chambers to Promote the Growth of Adipose Tissue. *Sci. Rep.* 2020, 10, 11779.
10. Wang, X.; Ao, Q.; Tian, X.; Fan, J.; Wei, Y.; Hou, W.; Tong, H.; Bai, S. 3D Bioprinting Technologies for Hard Tissue and Organ Engineering. *Materials* 2016, 9, 802.
11. Groll, J.; Burdick, J.A.; Cho, D.-W.; Derby, B.; Gelinsky, M.; Heilshorn, S.C.; Jüngst, T.; Malda, J.; Mironov, V.A.; Nakayama, K.; et al. A Definition of Bioinks and Their Distinction from Biomaterial Inks. *Biofabrication* 2018, 11, 013001.
12. Murphy, S.V.; Coppi, P.D.; Atala, A. Opportunities and Challenges of Translational 3D Bioprinting. *Nat. Biomed. Eng.* 2020, 4, 370–380.
13. Boland, T.; Mironov, V.; Gutowska, A.; Roth, E.A.; Markwald, R.R. Cell and Organ Printing 2: Fusion of Cell Aggregates in Three-dimensional Gels. *Anat. Rec. Part A Discov. Mol. Cell. Evol. Biol.* 2003, 272, 497–502.
14. Ventura, R.D. An Overview of Laser-Assisted Bioprinting (LAB) in Tissue Engineering Applications. *Med. Lasers* 2021, 10, 76–81.
15. Dou, C.; Perez, V.; Qu, J.; Tsin, A.; Xu, B.; Li, J. A State-of-the-Art Review of Laser-Assisted Bioprinting and Its Future Research Trends. *ChemBioEng Rev.* 2021, 8, 517–534.

16. Li, X.; Liu, B.; Pei, B.; Chen, J.; Zhou, D.; Peng, J.; Zhang, X.; Jia, W.; Xu, T. Inkjet Bioprinting of Biomaterials. *Chem. Rev.* 2020, 120, 10596–10636.
17. Kumar, P.; Ebbens, S.; Zhao, X. Inkjet Printing of Mammalian Cells—Theory and Applications. *Bioprinting* 2021, 23, e00157.
18. Ramesh, S.; Zhang, Y.; Cormier, D.R.; Rivero, I.V.; Harrysson, O.L.A.; Rao, P.K.; Tamayol, A.; Tamayol, A. Extrusion Bioprinting: Recent Progress, Challenges, and Future Opportunities. *Bioprinting* 2020, 21, e00116.
19. Zhang, Y.S.; Haghighashtiani, G.; Hübscher, T.; Kelly, D.J.; Lee, J.M.; Lutolf, M.; McAlpine, M.C.; Yeong, W.Y.; Zenobi-Wong, M.; Malda, J. 3D Extrusion Bioprinting. *Nat. Rev. Methods Primers* 2021, 1, 75.
20. Cui, X.; Li, J.; Hartanto, Y.; Durham, M.; Tang, J.; Zhang, H.; Hooper, G.; Lim, K.; Woodfield, T. Advances in Extrusion 3D Bioprinting: A Focus on Multicomponent Hydrogel-Based Bioinks. *Adv. Healthc. Mater.* 2020, 9, 1901648.
21. Zheng, Z.; Eglin, D.; Alini, M.; Richards, G.R.; Qin, L.; Lai, Y. Visible Light-Induced 3D Bioprinting Technologies and Corresponding Bioink Materials for Tissue Engineering: A Review. *Engineering* 2020, 7, 966–978.
22. Kilian, D.; Ahlfeld, T.; Akkineni, A.R.; Lode, A.; Gelinsky, M. Three-Dimensional Bioprinting of Volumetric Tissues and Organs. *Mrs. Bull.* 2017, 42, 585–592.
23. Wang, M.; Li, W.; Mille, L.S.; Ching, T.; Luo, Z.; Tang, G.; Garciamendez, C.E.; Lesha, A.; Hashimoto, M.; Zhang, Y.S. Digital Light Processing Based Bioprinting with Composable Gradients. *Adv. Mater.* 2022, 34, 2107038.
24. Bernal, P.N.; Delrot, P.; Loterie, D.; Li, Y.; Malda, J.; Moser, C.; Levato, R. Volumetric Bioprinting of Complex Living-Tissue Constructs within Seconds. *Adv. Mater.* 2019, 31, e1904209.
25. Li, J.; Parra-Cantu, C.; Wang, Z.; Zhang, Y.S. Improving Bioprinted Volumetric Tumor Microenvironments In Vitro. *Trends Cancer* 2020, 6, 745–756.
26. Gudapati, H.; Dey, M.; Ozbolat, I. A Comprehensive Review on Droplet-Based Bioprinting: Past, Present and Future. *Biomaterials* 2016, 102, 20–42.
27. Jentsch, S.; Nasehi, R.; Kuckelkorn, C.; Gundert, B.; Aveic, S.; Fischer, H. Multiscale 3D Bioprinting by Nozzle-Free Acoustic Droplet Ejection. *Small Methods* 2021, 5, 2000971.
28. Ng, W.L.; Lee, J.M.; Yeong, W.Y.; Naing, M.W. Microvalve-Based Bioprinting—Process, Bio-Inks and Applications. *Biomater. Sci.* 2017, 5, 632–647.
29. Costa, E.C.; Moreira, A.F.; de Melo-Diogo, D.; Gaspar, V.M.; Carvalho, M.P.; Correia, I.J. 3D Tumor Spheroids: An Overview on the Tools and Techniques Used for Their Analysis. *Biotechnol. Adv.* 2016, 34, 1427–1441.
30. Pinto, B.; Henriques, A.C.; Silva, P.M.A.; Bousbaa, H. Three-Dimensional Spheroids as In Vitro Preclinical Models for Cancer Research. *Pharmaceutics* 2020, 12, 1186.
31. Friedrich, J.; Seidel, C.; Ebner, R.; Kunz-Schughart, L.A. Spheroid-Based Drug Screen: Considerations and Practical Approach. *Nat. Protoc.* 2009, 4, 309–324.
32. Zaroni, M.; Piccinini, F.; Arienti, C.; Zamagni, A.; Santi, S.; Polico, R.; Bevilacqua, A.; Tesei, A. 3D Tumor Spheroid Models for in Vitro Therapeutic Screening: A Systematic Approach to Enhance the Biological Relevance of Data Obtained. *Sci. Rep.* 2016, 6, 19103.
33. Ma, H.; Jiang, Q.; Han, S.; Wu, Y.; Tomshine, J.C.; Wang, D.; Gan, Y.; Zou, G.; Liang, X.-J. Multicellular Tumor Spheroids as an in Vivo-Like Tumor Model for Three-Dimensional Imaging of Chemotherapeutic and Nano Material Cellular Penetration. *Mol. Imaging* 2012, 11, 7290.2012.00012.
34. Longati, P.; Jia, X.; Eimer, J.; Wagman, A.; Witt, M.-R.; Rehnmark, S.; Verbeke, C.; Toftgård, R.; Löhr, M.; Heuchel, R.L. 3D Pancreatic Carcinoma Spheroids Induce a Matrix-Rich, Chemoresistant Phenotype Offering a Better Model for Drug Testing. *BMC Cancer* 2013, 13, 95.
35. Loebbecke, A.B.; Halberstadt, C.R.; Holder, W.D.; Culberson, C.R.; Beiler, R.J.; Greene, K.G.; Roland, W.D.; Burg, K.J.L. The Development of an Embedding Technique for Polylactide Sponges. *J. Biomed. Mater. Res.* 1999, 48, 504–510.
36. Ruan, J.-L.; Tulloch, N.L.; Muskheli, V.; Genova, E.E.; Mariner, P.D.; Anseth, K.S.; Murry, C.E. An Improved Cryosection Method for Polyethylene Glycol Hydrogels Used in Tissue Engineering. *Tissue Eng. Part C Methods* 2013, 19, 794–801.
37. James, R.; Jenkins, L.; Ellis, S.E.; Burg, K.J.L. Histological Processing of Hydrogel Scaffolds for Tissue-Engineering Applications. *J. Histotechnol.* 2004, 27, 133–139.
38. Bédier, A.; Piacentini, N.; Aeberli, L.; Silva, A.D.; Verheyen, C.A.; Bonini, F.; Rochat, A.; Filippova, A.; Serex, L.; Renaud, P.; et al. Additive Manufacturing of Hierarchical Injectable Scaffolds for Tissue Engineering. *Acta Biomater.* 2018, 76, 71–79.

39. Huisken, J.; Swoger, J.; Bene, F.D.; Wittbrodt, J.; Stelzer, E.H.K. Optical Sectioning Deep Inside Live Embryos by Selective Plane Illumination Microscopy. *Science* 2004, 305, 1007–1009.
40. Schneckenburger, H.; Weber, P.; Wagner, M.; Schickinger, S.; Richter, V.; Bruns, T.; Strauss, W.S.I.; Wittig, R. Light Exposure and Cell Viability in Fluorescence Microscopy. *J. Microsc.* 2012, 245, 311–318.
41. Smyrek, I.; Stelzer, E.H.K. Quantitative Three-Dimensional Evaluation of Immunofluorescence Staining for Large Whole Mount Spheroids with Light Sheet Microscopy. *Biomed. Opt. Express* 2017, 8, 484–499.
42. Lazzari, G.; Vinciguerra, D.; Balasso, A.; Nicolas, V.; Goudin, N.; Garfa-Traore, M.; Fehér, A.; Dinnyés, A.; Nicolas, J.; Couvreur, P.; et al. Light Sheet Fluorescence Microscopy versus Confocal Microscopy: In Quest of a Suitable Tool to Assess Drug and Nanomedicine Penetration into Multicellular Tumor Spheroids. *Eur. J. Pharm. Biopharm.* 2019, 142, 195–203.
43. Yu, F.; Han, X.; Zhang, K.; Dai, B.; Shen, S.; Gao, X.; Teng, H.; Wang, X.; Li, L.; Ju, H.; et al. Evaluation of a Polyvinyl Alcohol-Alginate Based Hydrogel for Precise 3D Bioprinting. *J. Biomed. Mater. Res. A* 2018, 106, 2944–2954.
44. Li, X.; Chen, S.; Li, J.; Wang, X.; Zhang, J.; Kawazoe, N.; Chen, G. 3D Culture of Chondrocytes in Gelatin Hydrogels with Different Stiffness. *Polymers* 2016, 8, 269.
45. Cambria, E.; Brunner, S.; Heusser, S.; Fisch, P.; Hitzl, W.; Ferguson, S.J.; Wuertz-Kozak, K. Cell-Laden Agarose-Collagen Composite Hydrogels for Mechanotransduction Studies. *Front. Bioeng. Biotechnol.* 2020, 8, 346.
46. Axpe, E.; Oyen, M.L. Applications of Alginate-Based Bioinks in 3D Bioprinting. *Int. J. Mol. Sci.* 2016, 17, 1976.
47. Schmid, R.; Schmidt, S.K.; Hazur, J.; Detsch, R.; Maurer, E.; Boccaccini, A.R.; Hauptstein, J.; Teßmar, J.; Blunk, T.; Schrüfer, S.; et al. Comparison of Hydrogels for the Development of Well-Defined 3D Cancer Models of Breast Cancer and Melanoma. *Cancers* 2020, 12, 2320.
48. Qiao, S.; Zhao, Y.; Li, C.; Yin, Y.; Meng, Q.; Lin, F.-H.; Liu, Y.; Hou, X.; Guo, K.; Chen, X.; et al. An Alginate-Based Platform for Cancer Stem Cell Research. *Acta Biomater.* 2016, 37, 83–92.
49. Piras, C.C.; Smith, D.K. Multicomponent Polysaccharide Alginate-Based Bioinks. *J. Mater. Chem. B* 2020, 8, 8171–8188.
50. Jiang, T.; Munguia-Lopez, J.G.; Gu, K.; Bavoux, M.M.; Flores-Torres, S.; Kort-Mascort, J.; Grant, J.; Vijayakumar, S.; Leon-Rodriguez, A.D.; Ehrlicher, A.J.; et al. Engineering Bioprintable Alginate/Gelatin Composite Hydrogels with Tunable Mechanical and Cell Adhesive Properties to Modulate Tumor Spheroid Growth Kinetics. *Biofabrication* 2020, 12, 015024.
51. Reig-Vano, B.; Tylkowski, B.; Montané, X.; Giamberini, M. Alginate-Based Hydrogels for Cancer Therapy and Research. *Int. J. Biol. Macromol.* 2020, 170, 424–436.
52. Abasalizadeh, F.; Moghaddam, S.V.; Alizadeh, E.; akbari, E.; Kashani, E.; Fazljou, S.M.B.; Torbati, M.; Akbarzadeh, A. Alginate-Based Hydrogels as Drug Delivery Vehicles in Cancer Treatment and Their Applications in Wound Dressing and 3D Bioprinting. *J. Biol. Eng.* 2020, 14, 8.
53. Ying, G.; Jiang, N.; Yu, C.; Zhang, Y.S. Three-Dimensional Bioprinting of Gelatin Methacryloyl (GelMA). *Bio-Des. Manuf.* 2018, 1, 215–224.
54. He, H.; Li, D.; Lin, Z.; Peng, L.; Yang, J.; Wu, M.; Cheng, D.; Pan, H.; Ruan, C. Temperature-Programmable and Enzymatically Solidifiable Gelatin-Based Bioinks Enable Facile Extrusion Bioprinting. *Biofabrication* 2020, 12, 045003.
55. Rajabi, N.; Rezaei, A.; Kharaziha, M.; Bakhsheshi-Rad, H.R.; Luo, H.; RamaKrishna, S.; Berto, F. Recent Advances on Bioprinted Gelatin Methacrylate-Based Hydrogels for Tissue Repair. *Tissue Eng. Part A* 2021, 27, 679–702.
56. Yue, K.; Santiago, G.T.; Alvarez, M.M.; Tamayol, A.; Annabi, N.; Khademhosseini, A. Synthesis, Properties, and Biomedical Applications of Gelatin Methacryloyl (GelMA) Hydrogels. *Biomaterials* 2015, 73, 254–271.
57. Mao, S.; He, J.; Zhao, Y.; Liu, T.; Xie, F.; Yang, H.; Mao, Y.; Pang, Y.; Sun, W. Bioprinting of Patient-Derived in Vitro Intrahepatic Cholangiocarcinoma Tumor Model: Establishment, Evaluation and Anti-Cancer Drug Testing. *Biofabrication* 2020, 12, 045014.
58. Miranda, M.A.; Marcato, P.D.; Mondal, A.; Chowdhury, N.; Gebeyehu, A.; Surapaneni, S.K.; Bentley, M.V.L.B.; Amaral, R.; Pan, C.-X.; Singh, M. Cytotoxic and Chemosensitizing Effects of Glycoalkaloidic Extract on 2D and 3D Models Using RT4 and Patient Derived Xenografts Bladder Cancer Cells. *Mater. Sci. Eng. C* 2021, 119, 111460.
59. Piras, C.C.; Fernández-Prieto, S.; Borggraeve, W.M.D. Nanocellulosic Materials as Bioinks for 3D Bioprinting. *Biomater. Sci.* 2017, 5, 1988–1992.
60. Wang, X.; Wang, Q.; Xu, C. Nanocellulose-Based Inks for 3D Bioprinting: Key Aspects in Research Development and Challenging Perspectives in Applications—A Mini Review. *Bioengineering* 2020, 7, 40.

61. Kim, J.; Jang, J.; Cho, D.-W. Controlling Cancer Cell Behavior by Improving the Stiffness of Gastric Tissue-Decellularized ECM Bioink With Cellulose Nanoparticles. *Front. Bioeng. Biotechnol.* 2021, 9, 605819.
62. Gospodinova, A.; Nankov, V.; Tomov, S.; Redzheb, M.; Petrov, P.D. Extrusion Bioprinting of Hydroxyethylcellulose-Based Bioink for Cervical Tumor Model. *Carbohydr. Polym.* 2021, 260, 117793.
63. Olmos-Juste, R.; Alonso-Lerma, B.; Pérez-Jiménez, R.; Gabilondo, N.; Eceiza, A. 3D Printed Alginate-Cellulose Nanofibers Based Patches for Local Curcumin Administration. *Carbohydr. Polym.* 2021, 264, 118026.
64. Stefano, P.D.; Briatico-Vangosa, F.; Bianchi, E.; Pellegata, A.F.; de Hartungen, A.H.; Corti, P.; Dubini, G. Bioprinting of Matrigel Scaffolds for Cancer Research. *Polymers* 2021, 13, 2026.
65. Fan, R.; Piou, M.; Darling, E.; Cormier, D.; Sun, J.; Wan, J. Bio-Printing Cell-Laden Matrigel–Agarose Constructs. *J. Biomater. Appl.* 2016, 31, 684–692.
66. Snyder, J.E.; Hamid, Q.; Wang, C.; Chang, R.; Emami, K.; Wu, H.; Sun, W. Bioprinting Cell-Laden Matrigel for Radioprotection Study of Liver by pro-Drug Conversion in a Dual-Tissue Microfluidic Chip. *Biofabrication* 2011, 3, 034112.
67. Horváth, L.; Umehara, Y.; Jud, C.; Blank, F.; Petri-Fink, A.; Rothen-Rutishauser, B. Engineering an in Vitro Air-Blood Barrier by 3D Bioprinting. *Sci. Rep.* 2015, 5, 7974.
68. Benton, G.; Kleinman, H.K.; George, J.; Arnaoutova, I. Multiple Uses of Basement Membrane-like Matrix (BME/Matrigel) in Vitro and in Vivo with Cancer Cells. *Int. J. Cancer* 2011, 128, 1751–1757.
69. Osidak, E.O.; Kozhukhov, V.I.; Osidak, M.S.; Domogatsky, S.P. Collagen as Bioink for Bioprinting: A Comprehensive Review. *Int. J. Bioprint.* 2020, 6, 270.
70. Swaminathan, S.; Hamid, Q.; Sun, W.; Clyne, A.M. Bioprinting of 3D Breast Epithelial Spheroids for Human Cancer Models. *Biofabrication* 2019, 11, 025003.
71. Marques, C.F.; Diogo, G.S.; Pina, S.; Oliveira, J.M.; Silva, T.H.; Reis, R.L. Collagen-Based Bioinks for Hard Tissue Engineering Applications: A Comprehensive Review. *J. Mater. Sci. Mater. Med.* 2019, 30, 32.
72. Campos, D.F.D.; Marquez, A.B.; O’Seanain, C.; Fischer, H.; Blaeser, A.; Vogt, M.; Corallo, D.; Aveic, S. Exploring Cancer Cell Behavior In Vitro in Three-Dimensional Multicellular Bioprintable Collagen-Based Hydrogels. *Cancers* 2019, 11, 180.
73. Noh, I.; Kim, N.; Tran, H.N.; Lee, J.; Lee, C. 3D Printable Hyaluronic Acid-Based Hydrogel for Its Potential Application as a Bioink in Tissue Engineering. *Biomater. Res.* 2019, 23, 3.
74. Schmid, R.; Schmidt, S.K.; Detsch, R.; Horder, H.; Blunk, T.; Schrüfer, S.; Schubert, D.W.; Fischer, L.; Thievensen, I.; Heltmann-Meyer, S.; et al. A New Printable Alginate/Hyaluronic Acid/Gelatin Hydrogel Suitable for Biofabrication of In Vitro and In Vivo Metastatic Melanoma Models. *Adv. Funct. Mater.* 2021, 32, 2107993.
75. Petta, D.; D’Amora, U.; Ambrosio, L.; Grijpma, D.W.; Eglin, D.; D’Este, M. Hyaluronic Acid as a Bioink for Extrusion-Based 3D Printing. *Biofabrication* 2020, 12, 032001.
76. Horder, H.; Lasheras, M.G.; Grummel, N.; Nadernezhad, A.; Herbig, J.; Ergün, S.; Teßmar, J.; Groll, J.; Fabry, B.; Bauer-Kreisel, P.; et al. Bioprinting and Differentiation of Adipose-Derived Stromal Cell Spheroids for a 3D Breast Cancer-Adipose Tissue Model. *Cells* 2021, 10, 803.
77. López-Marcial, G.R.; Zeng, A.Y.; Osuna, C.; Dennis, J.; García, J.M.; O’Connell, G.D. Agarose-Based Hydrogels as Suitable Bioprinting Materials for Tissue Engineering. *ACS Biomater. Sci. Eng.* 2018, 4, 3610–3616.
78. Kim, J.E.; Kim, S.H.; Jung, Y. Current Status of Three-Dimensional Printing Inks for Soft Tissue Regeneration. *Tissue Eng. Regen. Med.* 2016, 13, 636–646.
79. Abelseth, E.; Abelseth, L.; la Vega, L.D.; Beyer, S.T.; Wadsworth, S.J.; Willerth, S.M. 3D Printing of Neural Tissues Derived from Human Induced Pluripotent Stem Cells Using a Fibrin-Based Bioink. *ACS Biomater. Sci. Eng.* 2019, 5, 234–243.
80. Lee, C.; Abelseth, E.; de la Vega, L.; Willerth, S.M. Bioprinting a Novel Glioblastoma Tumor Model Using a Fibrin-Based Bioink for Drug Screening. *Mater. Today Chem.* 2019, 12, 78–84.
81. Sharma, R.; Smits, I.P.M.; Vega, L.D.L.; Lee, C.; Willerth, S.M. 3D Bioprinting Pluripotent Stem Cell Derived Neural Tissues Using a Novel Fibrin Bioink Containing Drug Releasing Microspheres. *Front. Bioeng. Biotechnol.* 2020, 8, 57.
82. Chawla, S.; Midha, S.; Sharma, A.; Ghosh, S. Silk-Based Bioinks for 3D Bioprinting. *Adv. Healthc. Mater.* 2018, 7, 1701204.
83. Gangrade, A.; Mandal, B.B. Drug Delivery of Anticancer Drugs from Injectable 3D Porous Silk Scaffold for Prevention of Gastric Cancer Growth and Recurrence. *ACS Biomater. Sci. Eng.* 2020, 6, 6195–6206.

84. Qian, K.-Y.; Song, Y.; Yan, X.; Dong, L.; Xue, J.; Xu, Y.; Wang, B.; Cao, B.; Hou, Q.; Peng, W.; et al. Injectable Ferrimagnetic Silk Fibroin Hydrogel for Magnetic Hyperthermia Ablation of Deep Tumor. *Biomaterials* 2020, 259, 120299.
85. Wang, Q.; Han, G.; Yan, S.; Zhang, Q. 3D Printing of Silk Fibroin for Biomedical Applications. *Materials* 2019, 12, 504.
86. Pitarresi, G.; Martorana, A.; Palumbo, F.S.; Fiorica, C.; Giammona, G. New Gellan Gum-Graft-Poly(d,l-Lactide-co-Glycolide) Copolymers as Promising Bioinks: Synthesis and Characterization. *Int. J. Biol. Macromol.* 2020, 162, 1653–1667.
87. Zhu, S.; Yao, L.; Pan, C.; Tian, J.; Li, L.; Luo, B.; Zhou, C.; Lu, L. 3D Printed Gellan Gum/Graphene Oxide Scaffold for Tumor Therapy and Bone Reconstruction. *Compos. Sci. Technol.* 2021, 208, 108763.
88. Lozano, R.; Stevens, L.; Thompson, B.C.; Gilmore, K.J.; Gorkin, R.; Stewart, E.M.; in het Panhuis, M.; Romero-Ortega, M.; Wallace, G.G. 3D Printing of Layered Brain-like Structures Using Peptide Modified Gellan Gum Substrates. *Biomaterials* 2015, 67, 264–273.
89. Tonda-Turo, C.; Carmagnola, I.; Chiappone, A.; Feng, Z.; Ciardelli, G.; Hakkarainen, M.; Sangermano, M. Photocurable Chitosan as Bioink for Cellularized Therapies towards Personalized Scaffold Architecture. *Bioprinting* 2020, 18, e00082.
90. Babu, A.; Ramesh, R. Multifaceted Applications of Chitosan in Cancer Drug Delivery and Therapy. *Mar. Drugs* 2017, 15, 96.
91. Sahranavard, M.; Zamanian, A.; Ghorbani, F.; Shahrezaee, M.H. A Critical Review on Three Dimensional-Printed Chitosan Hydrogels for Development of Tissue Engineering. *Bioprinting* 2020, 17, e00063.
92. Roth, A.D.; Lama, P.; Dunn, S.; Hong, S.; Lee, M.-Y. Polymer Coating on a Micropillar Chip for Robust Attachment of PuraMatrix Peptide Hydrogel for 3D Hepatic Cell Culture. *Mater. Sci. Eng. C Mater. Biol. Appl.* 2018, 90, 634–644.
93. Yang, Z.; Xu, H.; Zhao, X. Designer Self-Assembling Peptide Hydrogels to Engineer 3D Cell Microenvironments for Cell Constructs Formation and Precise Oncology Remodeling in Ovarian Cancer. *Adv. Sci.* 2020, 7, 1903718.
94. Pati, F.; Jang, J.; Ha, D.-H.; Kim, S.W.; Rhie, J.-W.; Shim, J.-H.; Kim, D.-H.; Cho, D.-W. Printing Three-Dimensional Tissue Analogues with Decellularized Extracellular Matrix Bioink. *Nat. Commun.* 2014, 5, 3935.
95. Ferreira, L.P.; Gaspar, V.M.; Mano, J.F. Decellularized Extracellular Matrix for Bioengineering Physiometric 3D in Vitro Tumor Models. *Trends Biotechnol.* 2020, 38, 1397–1414.
96. Jang, J.; Park, H.-J.; Kim, S.-W.; Kim, H.; Park, J.Y.; Na, S.J.; Kim, H.J.; Park, M.N.; Choi, S.H.; Park, S.H.; et al. 3D Printed Complex Tissue Construct Using Stem Cell-Laden Decellularized Extracellular Matrix Bioinks for Cardiac Repair. *Biomaterials* 2017, 112, 264–274.
97. Hwang, J.; San, B.H.; Turner, N.J.; White, L.J.; Faulk, D.M.; Badylak, S.F.; Li, Y.; Yu, S.M. Molecular Assessment of Collagen Denaturation in Decellularized Tissues Using a Collagen Hybridizing Peptide. *Acta Biomater.* 2017, 53, 268–278.
98. He, Y.; Wang, F.; Wang, X.; Zhang, J.; Wang, D.; Huang, X. A Photocurable Hybrid Chitosan/Acrylamide Bioink for DLP Based 3D Bioprinting. *Mater. Des.* 2021, 202, 109588.
99. Poellmann, M.J.; Johnson, A.J.W. Multimaterial Polyacrylamide: Fabrication with Electrohydrodynamic Jet Printing, Applications, and Modeling. *Biofabrication* 2014, 6, 035018.
100. Poh, P.S.P.; Hutmacher, D.W.; Stevens, M.M.; Woodruff, M.A. Fabrication and in Vitro Characterization of Bioactive Glass Composite Scaffolds for Bone Regeneration. *Biofabrication* 2013, 5, 045005.
101. Kundu, J.; Shim, J.-H.; Jang, J.; Kim, S.-W.; Cho, D.-W. An Additive Manufacturing-Based PCL-Alginate-Chondrocyte Bioprinted Scaffold for Cartilage Tissue Engineering. *J. Tissue Eng. Regen. Med.* 2013, 9, 1286–1297.
102. Zamani, Y.; Mohammadi, J.; Amoabediny, G.; Helder, M.N.; Zandieh-Doulabi, B.; Klein-Nulend, J. Bioprinting of Alginate-Encapsulated Pre-Osteoblasts in PLGA/β-TCP Scaffolds Enhances Cell Retention but Impairs Osteogenic Differentiation Compared to Cell Seeding after 3D-Printing. *Regen. Eng. Transl. Med.* 2021, 7, 485–493.
103. Abelardo, E. *3D Bioprinting for Reconstructive Surgery*; Woodhead Publishing Series in Biomaterials; Elsevier: Amsterdam, The Netherlands, 2018; pp. 137–144.
104. Zhu, J. Bioactive Modification of Poly(Ethylene Glycol) Hydrogels for Tissue Engineering. *Biomaterials* 2010, 31, 4639–4656.
105. Hong, S.; Sycks, D.; Chan, H.F.; Lin, S.; Lopez, G.P.; Guilak, F.; Leong, K.W.; Zhao, X. 3D Printing of Highly Stretchable and Tough Hydrogels into Complex, Cellularized Structures. *Adv. Mater.* 2015, 27, 4035–4040.
106. Müller, M.; Becher, J.; Schnabelrauch, M.; Zenobi-Wong, M. Nanostructured Pluronic Hydrogels as Bioinks for 3D Bioprinting. *Biofabrication* 2015, 7, 035006.

107. Gioffredi, E.; Boffito, M.; Calzone, S.; Giannitelli, S.M.; Rainer, A.; Trombetta, M.; Mozetic, P.; Chiono, V. Pluronic F127 Hydrogel Characterization and Biofabrication in Cellularized Constructs for Tissue Engineering Applications. *Proc. Cirp.* 2016, 49, 125–132.
108. Hsieh, F.-Y.; Lin, H.-H.; Hsu, S. 3D Bioprinting of Neural Stem Cell-Laden Thermoresponsive Biodegradable Polyurethane Hydrogel and Potential in Central Nervous System Repair. *Biomaterials* 2015, 71, 48–57.
109. Hung, K.; Tseng, C.; Hsu, S. Synthesis and 3D Printing of Biodegradable Polyurethane Elastomer by a Water-Based Process for Cartilage Tissue Engineering Applications. *Adv. Healthc. Mater.* 2014, 3, 1578–1587.
110. Norberg, K.J.; Liu, X.; Moro, C.F.; Strell, C.; Nania, S.; Blümel, M.; Balboni, A.; Bozóky, B.; Heuchel, R.L.; Löhr, J.M. A Novel Pancreatic Tumour and Stellate Cell 3D Co-Culture Spheroid Model. *BMC Cancer* 2020, 20, 475.
111. Ewa-Choy, Y.W.; Pingguan-Murphy, B.; Abdul-Ghani, N.A.; Jahendran, J.; Chua, K.H. Effect of Alginate Concentration on Chondrogenesis of Co-Cultured Human Adipose-Derived Stem Cells and Nasal Chondrocytes: A Biological Study. *Biomater. Res.* 2017, 21, 19.
112. Li, X.; Chen, Y.; Kawazoe, N.; Chen, G. Influence of Microporous Gelatin Hydrogels on Chondrocyte Functions. *J. Mater. Chem. B* 2017, 5, 5753–5762.
113. Meinert, C.; Schrobback, K.; Hutmacher, D.W.; Klein, T.J. A Novel Bioreactor System for Biaxial Mechanical Loading Enhances the Properties of Tissue-Engineered Human Cartilage. *Sci. Rep.* 2017, 7, 16997.
114. Park, H.; Temenoff, J.S.; Tabata, Y.; Caplan, A.I.; Mikos, A.G. Injectable Biodegradable Hydrogel Composites for Rabbit Marrow Mesenchymal Stem Cell and Growth Factor Delivery for Cartilage Tissue Engineering. *Biomaterials* 2007, 28, 3217–3227.
115. Haugh, M.G.; Meyer, E.G.; Thorpe, S.D.; Vinardell, T.; Duffy, G.P.; Kelly, D.J. Temporal and Spatial Changes in Cartilage-Matrix-Specific Gene Expression in Mesenchymal Stem Cells in Response to Dynamic Compression. *Tissue Eng. Part A* 2011, 17, 3085–3093.
116. Gauch, S.; Hermann, R.; Feuser, P.; Oelmüller, U.; Bastian, H. Isolation of Total RNA Using Silica-Gel Based Membranes. In *Molecular Tools for Screening Biodiversity: Plants and Animals*; Karp, I.A., Ingram, P.G., David, S., Eds.; Springer: Dordrecht, The Netherlands, 1998; pp. 67–70.
117. Köster, N.; Schmiermund, A.; Grubelnig, S.; Leber, J.; Ehlicke, F.; Czermak, P.; Salzig, D. Single-Step RNA Extraction from Different Hydrogel-Embedded Mesenchymal Stem Cells for Quantitative Reverse Transcription–Polymerase Chain Reaction Analysis. *Tissue Eng. Part C Methods* 2016, 22, 552–560.
118. Bougault, C.; Paumier, A.; Aubert-Foucher, E.; Mallein-Gerin, F. Investigating Conversion of Mechanical Force into Biochemical Signaling in Three-Dimensional Chondrocyte Cultures. *Nat. Protoc.* 2009, 4, 928–938.
119. Sbrana, F.V.; Pinos, R.; Barbaglio, F.; Ribezzi, D.; Scagnoli, F.; Scarfò, L.; Redwan, I.N.; Martinez, H.; Farè, S.; Ghia, P.; et al. 3D Bioprinting Allows the Establishment of Long-Term 3D Culture Model for Chronic Lymphocytic Leukemia Cells. *Front. Immunol.* 2021, 12, 639572.
120. Shin, D.-S.; You, J.; Rahimian, A.; Vu, T.; Siltanen, C.; Ehsanipour, A.; Stybayeva, G.; Sutcliffe, J.; Revzin, A. Photodegradable Hydrogels for Capture, Detection, and Release of Live Cells. *Angew. Chem. Int. Ed.* 2014, 53, 8221–8224.
121. Friedrich, J.; Eder, W.; Castaneda, J.; Doss, M.; Huber, E.; Ebner, R.; Kunz-Schughart, L.A. A Reliable Tool to Determine Cell Viability in Complex 3-D Culture: The Acid Phosphatase Assay. *J. Biomol. Screen.* 2007, 12, 925–937.
122. Beaumont, K.A.; Anfosso, A.; Ahmed, F.; Weninger, W.; Haass, N.K. Imaging- and Flow Cytometry-Based Analysis of Cell Position and the Cell Cycle in 3D Melanoma Spheroids. *J. Vis. Exp.* 2015, 106, 53486.
123. Geng, Z.; Zhang, H.; Xiong, Q.; Zhang, Y.; Zhao, H.; Wang, G. A Fluorescent Chitosan Hydrogel Detection Platform for the Sensitive and Selective Determination of Trace Mercury(II) in Water. *J. Mater. Chem. A* 2015, 3, 19455–19460.
124. Khattak, S.F.; Spataro, M.; Roberts, L.; Roberts, S.C. Application of Colorimetric Assays to Assess Viability, Growth and Metabolism of Hydrogel-Encapsulated Cells. *Biotechnol. Lett.* 2006, 28, 1361–1370.
125. Polley, C.; Mau, R.; Lieberwirth, C.; Stenzel, J.; Vollmar, B.; Seitz, H. Bioprinting of Three Dimensional Tumor Models: A Preliminary Study Using a Low Cost 3D Printer. *Curr. Dir. Biomed. Eng.* 2017, 3, 135–138.
126. Ho, W.Y.; Yeap, S.K.; Ho, C.L.; Rahim, R.A.; Alitheen, N.B. Development of Multicellular Tumor Spheroid (MCTS) Culture from Breast Cancer Cell and a High Throughput Screening Method Using the MTT Assay. *PLoS ONE* 2012, 7, e44640.
127. Hunnewell, M.; Forbes, N.S. Active and Inactive Metabolic Pathways in Tumor Spheroids: Determination by GC-MS. *Biotechnol. Prog.* 2010, 26, 789–796.

128. Klapa, M.I.; Aon, J.-C.; Stephanopoulos, G. Ion-Trap Mass Spectrometry Used in Combination with Gas Chromatography for High-Resolution Metabolic Flux Determination. *Biotechniques* 2003, 34, 832–849.
129. Forbes, N.S.; Meadows, A.L.; Clark, D.S.; Blanch, H.W. Estradiol Stimulates the Biosynthetic Pathways of Breast Cancer Cells: Detection by Metabolic Flux Analysis. *Metab. Eng.* 2006, 8, 639–652.
130. Kim, B.; Forbes, N.S. Flux Analysis Shows That Hypoxia-Inducible-Factor-1-Alpha Minimally Affects Intracellular Metabolism in Tumor Spheroids. *Biotechnol. Bioeng.* 2007, 96, 1167–1182.
131. Tondera, C.; Hauser, S.; Krüger-Genge, A.; Jung, F.; Neffe, A.T.; Lendlein, A.; Klopffleisch, R.; Steinbach, J.; Neuber, C.; Pietzsch, J. Gelatin-Based Hydrogel Degradation and Tissue Interaction in Vivo: Insights from Multimodal Preclinical Imaging in Immunocompetent Nude Mice. *Theranostics* 2016, 6, 2114–2128.
132. Noel, P.; Muñoz, R.; Rogers, G.W.; Neilson, A.; Hoff, D.D.V.; Han, H. Preparation and Metabolic Assay of 3-Dimensional Spheroid Co-Cultures of Pancreatic Cancer Cells and Fibroblasts. *J. Vis. Exp. Jove.* 2017, 126, e56081.
133. Marchetti, P.; Fovez, Q.; Germain, N.; Khamari, R.; Kluza, J. Mitochondrial Spare Respiratory Capacity: Mechanisms, Regulation, and Significance in Non-Transformed and Cancer Cells. *FASEB J.* 2020, 34, 13106–13124.
134. Muir, A.; Danai, L.V.; Heiden, M.G.V. Microenvironmental Regulation of Cancer Cell Metabolism: Implications for Experimental Design and Translational Studies. *Dis. Model. Mech.* 2018, 11, dmm035758.
135. Mueller, M.M.; Fusenig, N.E. Friends or Foes—Bipolar Effects of the Tumour Stroma in Cancer. *Nat. Rev. Cancer* 2004, 4, 839–849.
136. Hanahan, D.; Coussens, L.M. Accessories to the Crime: Functions of Cells Recruited to the Tumor Microenvironment. *Cancer Cell* 2012, 21, 309–322.
137. Duong, M.N.; Geneste, A.; Fallone, F.; Li, X.; Dumontet, C.; Muller, C. The Fat and the Bad: Mature Adipocytes, Key Actors in Tumor Progression and Resistance. *Oncotarget* 2017, 8, 57622–57641.
138. Germain, N.; Dhayer, M.; Boileau, M.; Fovez, Q.; Kluza, J.; Marchetti, P. Lipid Metabolism and Resistance to Anticancer Treatment. *Biology* 2020, 9, 474.
139. Zhao, C.; Wu, M.; Zeng, N.; Xiong, M.; Hu, W.; Lv, W.; Yi, Y.; Zhang, Q.; Wu, Y. Cancer-Associated Adipocytes: Emerging Supporters in Breast Cancer. *J. Exp. Clin. Cancer Res.* 2020, 39, 156.
140. Sahai, E.; Astsaturov, I.; Cukierman, E.; DeNardo, D.G.; Egeblad, M.; Evans, R.M.; Fearon, D.; Greten, F.R.; Hingorani, S.R.; Hunter, T.; et al. A Framework for Advancing Our Understanding of Cancer-Associated Fibroblasts. *Nat. Rev. Cancer* 2020, 20, 174–186.
141. Fiori, M.E.; Franco, S.D.; Villanova, L.; Bianca, P.; Stassi, G.; Maria, R.D. Cancer-Associated Fibroblasts as Abettors of Tumor Progression at the Crossroads of EMT and Therapy Resistance. *Mol. Cancer* 2019, 18, 70.
142. Hanley, C.J.; Thomas, G.J. T-Cell Tumour Exclusion and Immunotherapy Resistance: A Role for CAF Targeting. *Br. J. Cancer* 2020, 123, 1353–1355.
143. Mondal, A.; Gebeyehu, A.; Miranda, M.; Bahadur, D.; Patel, N.; Ramakrishnan, S.; Rishi, A.K.; Singh, M. Characterization and Printability of Sodium Alginate -Gelatin Hydrogel for Bioprinting NSCLC Co-Culture. *Sci Rep.* 2019, 9, 19914.
144. Datta, P.; Dey, M.; Ataie, Z.; Unutmaz, D.; Ozbolat, I.T. 3D Bioprinting for Reconstituting the Cancer Microenvironment. *NPJ Precis. Oncol.* 2020, 4, 18.
145. Luo, Y.; Wei, X.; Huang, P. 3D Bioprinting of Hydrogel-based Biomimetic Microenvironments. *J. Biomed. Mater. Res. Part B Appl. Biomater.* 2019, 107, 1695–1705.
146. Samadian, H.; Jafari, S.; Sepand, M.R.; Alaei, L.; Malvajerd, S.S.; Jaymand, M.; Ghobadinezhad, F.; Jahanshahi, F.; Hamblin, M.R.; Derakhshankhah, H.; et al. 3D Bioprinting Technology to Mimic the Tumor Microenvironment: Tumor-on-a-Chip Concept. *Mater. Today Adv.* 2021, 12, 100160.
147. Albritton, J.L.; Miller, J.S. 3D Bioprinting: Improving in Vitro Models of Metastasis with Heterogeneous Tumor Microenvironments. *Dis. Model. Mech.* 2017, 10, 3–14.
148. Richards, D.; Jia, J.; Yost, M.; Markwald, R.; Mei, Y. 3D Bioprinting for Vascularized Tissue Fabrication. *Ann. Biomed. Eng.* 2017, 45, 132–147.
149. Rajabi, M.; Mousa, S.A. The Role of Angiogenesis in Cancer Treatment. *Biomedicines* 2017, 5, 34.
150. Liao, D.; Johnson, R.S. Hypoxia: A Key Regulator of Angiogenesis in Cancer. *Cancer Metast. Rev.* 2007, 26, 281–290.
151. Zervantonakis, I.K.; Hughes-Alford, S.K.; Charest, J.L.; Condeelis, J.S.; Gertler, F.B.; Kamm, R.D. Three-Dimensional Microfluidic Model for Tumor Cell Intravasation and Endothelial Barrier Function. *Proc. Natl. Acad. Sci. USA* 2012, 109, 13515–13520.

152. Meng, F.; Meyer, C.M.; Joung, D.; Valleria, D.A.; McAlpine, M.C.; Panoskaltsis-Mortari, A. 3D Bioprinted In Vitro Metastatic Models via Reconstruction of Tumor Microenvironments. *Adv. Mater.* 2019, 31, 1806899.
153. Chen, C.S. Mechanotransduction—a Field Pulling Together? *J. Cell Sci.* 2008, 121, 3285–3292.
154. Kulangara, K.; Leong, K.W. Substrate Topography Shapes Cell Function. *Soft Matter* 2009, 5, 4072–4076.
155. Ghibaudo, M.; Saez, A.; Trichet, L.; Xayaphoummine, A.; Browaeys, J.; Silberzan, P.; Buguin, A.; Ladoux, B. Traction Forces and Rigidity Sensing Regulate Cell Functions. *Soft Matter* 2008, 4, 1836–1843.
156. Orr, A.W.; Helmke, B.P.; Blackman, B.R.; Schwartz, M.A. Mechanisms of Mechanotransduction. *Dev. Cell* 2006, 10, 11–20.
157. Geiger, B.; Spatz, J.P.; Bershadsky, A.D. Environmental Sensing through Focal Adhesions. *Nat. Rev. Mol. Cell Biol.* 2009, 10, 21–33.
158. Baumgart, F. Stiffness—an Unknown World of Mechanical Science? *Injury* 2000, 31, 14–84.
159. Theocharis, A.D.; Skandalis, S.S.; Gialeli, C.; Karamanos, N.K. Extracellular Matrix Structure. *Adv. Drug Deliv. Rev.* 2016, 97, 4–27.
160. Ge, H.; Tian, M.; Pei, Q.; Tan, F.; Pei, H. Extracellular Matrix Stiffness: New Areas Affecting Cell Metabolism. *Front. Oncol.* 2021, 11, 631991.
161. Strickaert, A.; Saiselet, M.; Dom, G.; Deken, X.D.; Dumont, J.E.; Feron, O.; Sonveaux, P.; Maenhaut, C. Cancer Heterogeneity Is Not Compatible with One Unique Cancer Cell Metabolic Map. *Oncogene* 2017, 36, 2637–2642.

---

Retrieved from <https://encyclopedia.pub/entry/history/show/51482>